Wind and Structures, *Vol. 18, No. 1 (2014) 037-056*
DOI: http://dx.doi.org/10.12989/was.2014.18.1.037

Wind-tunnel tests on high-rise buildings: wind modes and structural response

Vincenzo Sepe* and Marcello Vasta[a]

Department of Engineering and Geology INGEO, University "G. D'Annunzio"
V.le Pindaro 42, I-65127 Pescara, Italy

(Received July 2, 2012, Revised June 25, 2013, Accepted August 26, 2013)

Abstract. The evaluation of pressure fields acting on slender structures under wind loads is currently performed in experimental aerodynamic tests. For wind-sensitive structures, in fact, the knowledge of global and local wind actions is crucial for design purpose. This paper considers a particular slender structure under wind excitation, representative of most common high-rise buildings, whose experimental wind field on in-scale model was measured in the CRIACIV boundary-layer wind tunnel (University of Florence) for several angles of attack of the wind. It is shown that an efficient reduced model to represent structural response can be obtained by coupling the classical structural modal projection with the so called blowing modes projection, obtained by decomposing the covariance or power spectral density (PSD) wind tensors. In particular, the elaboration of experimental data shows that the first few blowing modes can effectively represent the wind-field when eigenvectors of the PSD tensor are used, while a significantly larger number of blowing modes is required when the covariance wind tensor is used to decompose the wind field.

Keywords: slender structures; wind blowing modes; covariance proper transformation; spectral proper transformation; boundary layer wind-tunnel

1. Introduction

The evaluation of pressure fields acting on slender structures under wind loads is currently performed in experimental aerodynamic tests. For wind-sensitive structures, in fact, the question of representing global and local wind actions for design purpose is an important aspect in modern structural design. The main problem in this regard is the random nature of wind loads due to the presence of turbulence in the incoming flow. Therefore, statistical analysis is necessary and multi-variate random process theory are utilized to represent wind action on structures, making use of some a priori assumptions such as ergodicity or stationarity. The problem of choosing an optimal basis to represent wind action on structures is an open question and different approaches and representations are nowadays available in literature (see e.g., Carassale and Marré Brunenghi 2011, Carassale *et al.* 2007, Solari *et al.* 2007, Kikuchi *et al.* 1997).

*Corresponding author, Associate Professor, E-mail: v.sepe@unich.it
[a] Associate Professor, E-mail: mvasta@unich.it

http://www.techno-press.org/?journal=was&subpage=8 ISSN: 1226-6116 (Print), 1598-6225 (Online)

In case of experimental evaluation of pressure fields, at the real scale or at the scale of a wind-tunnel model, the classical approach available in literature is the Principal Component Analysis (PCA) where the decomposition of the covariance matrix estimated from the measured wind field allows for representing the random pressure field as a sum of deterministic vectors (blowing modes), modulated by time dependent random coefficients called principal components. A less common but well established representation derives from the analysis of the pressure field in the frequency domain. In this context it has been shown (e.g., Di Paola 1998) that the random field may be represented decomposing the power spectral matrix estimated from the data. Since the power spectral matrix is a complex-valued Hermitian-symmetric matrix, its complex eigenvectors are mutually orthogonal, while the eigenvalues are real and non-negative. The random pressure field can be represented as a sum of complex vectors (complex blowing modes), modulated by time dependent complex random coefficients, and this modal representation is referred to as Spectral Proper Transformation (SPT). The two representations are alternative, although not equivalent because SPT fully decorrelates the principal components, while PCA decorrelates them only for $\tau = 0$.

In this paper, particular attention has been devoted to reduced models of the wind loads acting on slender structures and their response characterization. Starting from the now well accepted representation of the wind field by means of blowing modes (or wind modes), i.e., coherent wind fields characterized by highest energetic weights and stochastically orthogonal to each other (e.g., Kikuchi *et al.* 1997, Carassale 2005, Carassale *et al.* 2007, Carassale and Marré Brunenghi 2012, Holmes *et al.* 1997, Kho *et al.* 2002, Tamura *et al.* 1997, Tamura *et al.* 1999), an investigation has been performed that uses experimental results obtained by means of wind tunnels tests.

The sample case is shown in Fig. 1, where the experimental wind field on the sample building was measured in the CRIACIV (University of Florence) wind-tunnel laboratory (Spence *et al.* 2008, Spence *et al.* 2011) by means of about 200 pressure taps for several angle of incidence of the wind, and was then reduced to resulting forces and couples acting on the 74 floors. In Fig. 2 the measured forcing field is shown in four different time-steps.

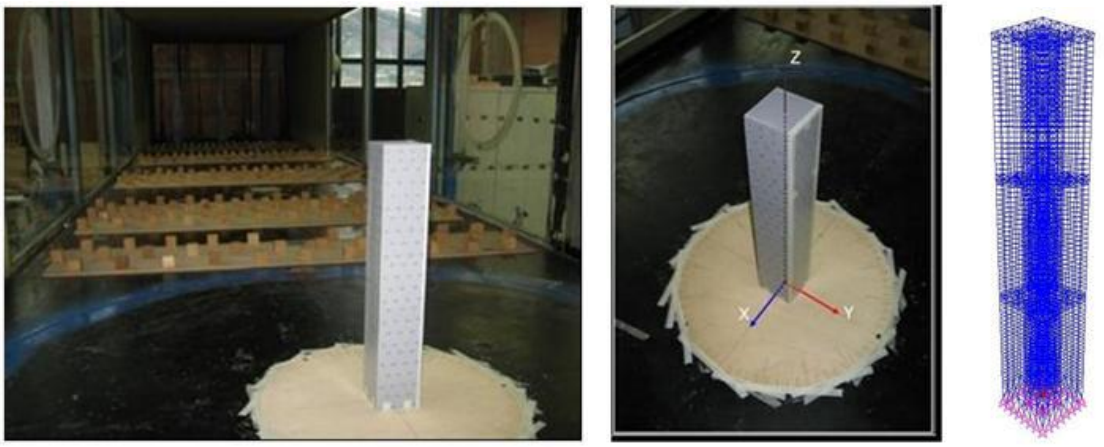

(a) (b) (c)

Fig. 1 (a)-(b) Wind-tunnel tests on in-scale model, CRIACIV boundary-layer wind tunnel in Prato (Italy) and (c) finite elements model (FEM) of the building assumed as a sample case.

Aiming to obtain a reduced model for the wind field, the paper describes two algorithms: the first extracts the wind-modes from the covariance matrix of the forcing time-histories, and represents them by means of a very expressive 3D representation; the second representation is instead obtained when eigenvectors of the power spectral density tensor are used, leading to a more precise frequency representation of the excitation load.

The elaboration of experimental data has shown that the multi-correlated field of wind-induced loads cannot in general be reduced to the contribution of the first few blowing modes of the covariance wind-tensor, because higher modes can play a non-negligible role, differently from what happens for the modal representation of the structure, that instead is satisfactorily reproduced by a truncated model with only the very first modes for slender structures. A more efficient reduction of the wind field is instead obtained when eigenvectors of the power spectral density tensor are used, and comparison to PCA representation is reported.

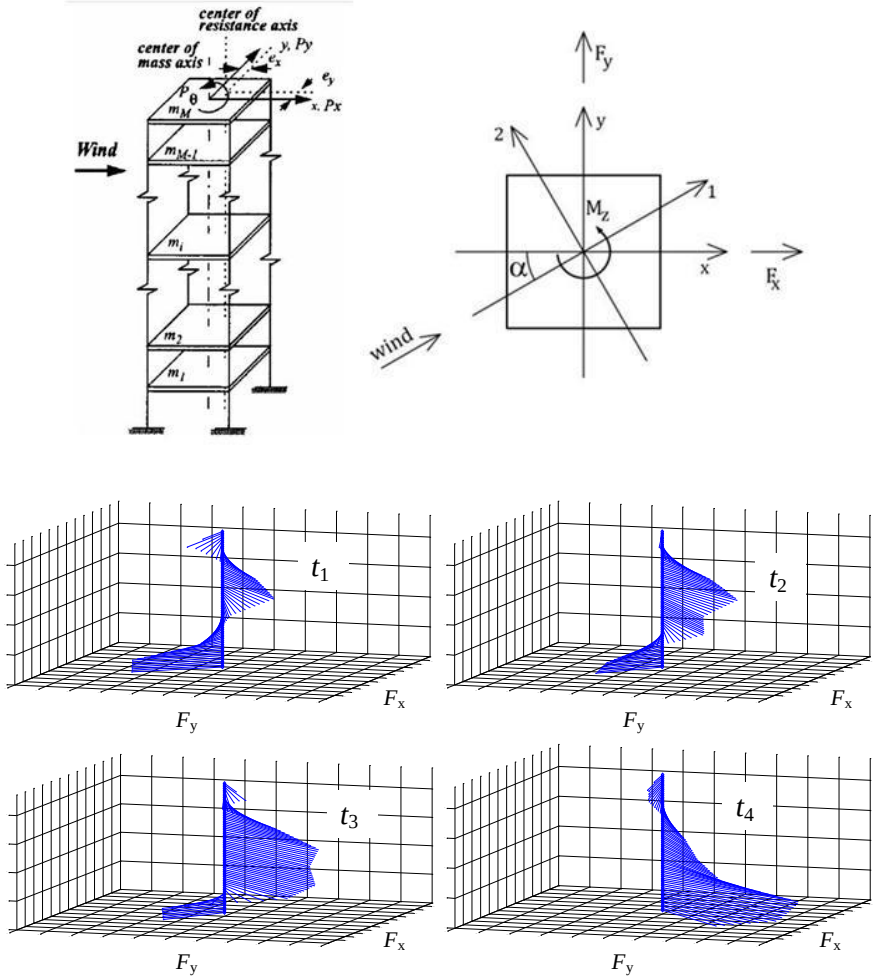

Fig. 2 Top: sketch of the building assumed as a sample case; Bottom: the measured forcing fields F_x, F_y, (couple M_z not represented) in four generic time-steps t_1,..., t_4

2. Wind-tunnel experimental tests and reduced structural model

In the framework of the research project "Wind effects on slender structures: Performance-based Optimal Design (Wi-POD)", funded by the Italian Ministry for University and Research and by five Italian Universities, wind-tunnel tests were performed on a 1:500 in-scale model of a high-rise building (Fig. 1), with dimensions 103.6 mm x 103.6 mm x 610.2 mm.

Measurements and their elaboration were performed by researchers of Florence and Perugia Universities (Spence 2009, Spence *et al.* 2011, Cluni *et al.* 2011) in the boundary-layer wind tunnel of CRIACIV (Inter-University Research Centre on Building Aerodynamics and Wind Engineering) in Prato (Italy).

The wind-field was measured for several angles of attack of the wind (0°, 10°, 20°, 30°, 40°, 45°) by means of about 200 pressure taps, with a power-law index $\bar{\alpha}$ = 1.6 of the mean wind speed profile.

The pressure field was then reduced to the resulting forces F_x, F_y and the couple M_z with respect to the centroid of each one of the 74 floors of the building.

The forcing field consists then of 222 (= 74 x 3) time-histories of the load components F_x, F_y, M_z.

The sampling rate was 250 Hz at the scale of the model and, depending on the scale factors (geometrical, wind speed, …), it corresponds to a sampling period of 0.84 seconds for wind time-histories representative of a return period of 50 years.

The structural analysis of slender structures, as the one herein considered, can be simplified if a modal projection is considered. Indeed, for this kind of structures, only few structural modes enables to represent the most important mechanical and structural characteristics. This was confirmed for the structure under investigation by FEM analysis. An FEM model of the building was developed (Fig. 1) and used for numerical simulations of the structural response under wind-induced loads. Due to the frequency content of the forcing field, the numerical simulation of the structural response is dominated by few structural modes and cannot include any significant contribution of the higher ones. This is made evident (Bellizzotti *et al.* 2010), for example, by the power spectral densities corresponding to the modal components of the forcing field (i.e., scalar product of the forcing field with each modal shape); they show in fact that only the first modal components of the wind-induced loads have a significant energy content around the frequency of the corresponding mode, while only a pair of modal components contribute with significant non-zero mean (i.e., "static" loads) to the structural response. Moreover, the contribution of flexural modal loads result, in the sample cases so far considered, much higher than the contribution of torsional modal components of the load.

As a consequence, a reduced model is considered in the following that includes only the first three modes, i.e., the first flexural mode in the x and y direction and the first torsional mode.

As well known, this allows to reduce the equations governing the motion to the following ones

$$\ddot{y}_j + 2\xi_j \omega_j \dot{y}_j + \omega_j^2 y_j = f_j(t) \qquad j = 1,2,3 \tag{1}$$

where ω_j and ξ_j are the frequency and damping coefficient of the j-th mode $\boldsymbol{\varphi}_j$, y_j denote the modal amplitudes and $f_j(t) = \boldsymbol{\varphi}_j^T \mathbf{F}(t)$ the modal components of the forcing field $\mathbf{F}(t)$, with modal masses taken as unity.

3. Reduced model of the wind-induced loads based on the covariance tensor

In the study of linear structures, the dynamic response is usually evaluated by applying modal analysis. The equations of motion are transformed from the initial Lagrangean space into the principal space where, under suitable conditions regarding the damping, the motion is ruled by decoupled equations expressed in terms of principal coordinates.

The main ingredient of this method is the selection of an appropriate coordinate system. It is well known that a suitable coordinate system can be established by the structural modes (eigenvectors) of the linear system that are most excited by the respective loading conditions. This is not the only possibility; however, it is usually a good choice.

On the other hand, even if modal analysis is assumed, the projection of the external wind load on the structural modes involves, because of cross correlations, a coupling between modes that are not statistically independent. A more suitable representation of the wind load can be obtained by considering a statistically consistent coordinate system. In contrast to the deterministic case, the probability density function (PDF) of the wind loading should be described by a low number of coordinates. The most essential characteristic of wind statistics are certainly its mean and second moments in terms of the covariance matrix. Therefore, a suitable coordinate system must be capable of representing the covariance matrix of the wind load. In the Karhunen-Loeve representation (the same concept is also known as principal component analysis, PCA), the eigenvectors of the covariance matrix associated with the largest eigenvalues lead to the best choice in the sense that the differences between the norms of the original covariance and the approximated matrices, respectively, are minimal. The PCA, based on the decomposition of the covariance response matrix, has been successfully applied in many areas, such as image decoding, physiology, climatology, and speech analysis (e.g., Honerkamp 1994).

The main idea of this technique consists in the evaluation of the wind process on an optimal basis, which coincides with the determination of the eigenvectors of the covariance matrix. In structural stochastic dynamics, PCA has been utilized mainly for simulation of stochastic fields (e.g., Yamazaki and Shinozuka 1990) and stochastic finite element analysis (e.g., Yamazaki *et al.* 1988; Ghanem and Spanos 1991, Vasta and Schueller 2000).

For the structure under examination, let $F_{xi}(t), F_{yi}(t), M_{zi}(t)$ be the resulting forces and torsional moment at the *i*-th floor, derived as resultant components of the measured pressure field. Denoting by *p* the number of floors ($p = 74$ in the sample case here discussed) the forcing components may be collected in a *m* x 1 vector process $\boldsymbol{F}(t)$, with $m = 3p$

$$\mathbf{F}(t) = \begin{bmatrix} F_{x1}(t) \\ F_{y1}(t) \\ M_1(t) \\ \vdots \\ F_{xp}(t) \\ F_{yp}(t) \\ M_p(t) \end{bmatrix} \tag{2}$$

The elements of the *m* x *m* covariance matrix $\mathbf{R}_{\mathbf{F}}(\tau) = \left[R_{F_i F_j}(\tau)\right]$ of the vector process $\mathbf{F}(t)$ are defined as

$$R_{F_iF_j}(\tau) = E\left[F_i(t)F_j(t+\tau)\right] - E\left[F_i(t)\right]E\left[F_j(t+\tau)\right] \qquad i, j = 1,..., m \tag{3}$$

The decomposition of the covariance matrix $\mathbf{R_F}(\tau) = [R_{FiFj}(\tau)]$ returns, for $\tau = 0$, the wind modes $\mathbf{\Phi} = [\boldsymbol{\phi}_1\ \boldsymbol{\phi}_2 \cdots \boldsymbol{\phi}_n]$, eigenvectors of $\mathbf{R} = \mathbf{R_F}(0)$, with associated eigenvalues $\mathbf{\Lambda} = diag(\lambda_1\ \lambda_2 \cdots \lambda_n)$

$$\mathbf{R\Phi} = \mathbf{\Phi\Lambda} \tag{4}$$

$$\mathbf{\Phi}^T\mathbf{\Phi} = \mathbf{I}, \quad \mathbf{\Phi}^T\mathbf{R\Phi} = \mathbf{\Lambda} \tag{5}$$

Thanks to these properties the covariance matrix $\mathbf{R}$ can be represented by the spectral decomposition

$$\mathbf{R} = \sum_{k=1}^{n} \boldsymbol{\phi}_k \boldsymbol{\phi}_k^T \lambda_k = \mathbf{\Phi\Lambda\Phi}^T \tag{6}$$

Following the idea of Karhunen and Loeve (see e.g., Loeve 1978), an optimal basis to represent the wind load ***F(t)*** is a linear combination of the wind modes $\boldsymbol{\phi}_k$ by the amplitude $g_k(t)$

$$\mathbf{F}(t) = \boldsymbol{\mu}_F + \sum_{k=1}^{m} \boldsymbol{\phi}_k g_k(t) = \boldsymbol{\mu}_F + \mathbf{\Phi}\,\mathbf{g}(t) \tag{7}$$

where $\boldsymbol{\mu}_F$ denotes the vector of mean forces.

In Eq. (7) the $g_k(t)$ are zero-mean stationary vector processes whose components are referred to as covariance principal components. Combining Eqs. (5) and (4) yields

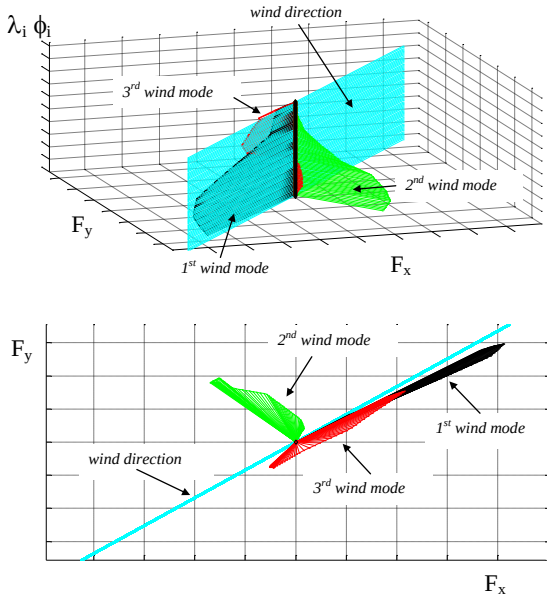

Fig. 3 Top: first three wind modes of covariance tensor **R** for the forcing field corresponding to angle of attack $\alpha = 40°$ (torsional component not represented); Bottom: projection on the plane F_x-F_y

$$\mathrm{E}\left[\mathbf{g}(\mathrm{t}+\tau)\mathbf{g}^{T}(\mathrm{t})\right]=\begin{cases}\boldsymbol{\Lambda} & \text{if } \tau=0\\ \boldsymbol{\Phi}^{T}\boldsymbol{R}_{F}(\tau)\boldsymbol{\Phi} & \text{otherwise}\end{cases} \tag{8}$$

It is worth noting that since measurement of $\mathbf{F}(t)$ are known in the case here described, the $g_k(t)$ processes can be evaluated by Eq. (7) using the orthogonality properties of the wind modes ϕ_k

$$g_k(t)=\boldsymbol{\phi}_k^{T}\left(\mathbf{F}(t)-\boldsymbol{\mu}_F\right) \tag{9}$$

If the eigenvalues are sorted in decreasing order, then the summation in Eq. (7) can be truncated considering only a limited number of principal components. In the case here considered, the covariance matrix is of order 222 (3 resulting force components for each floor).

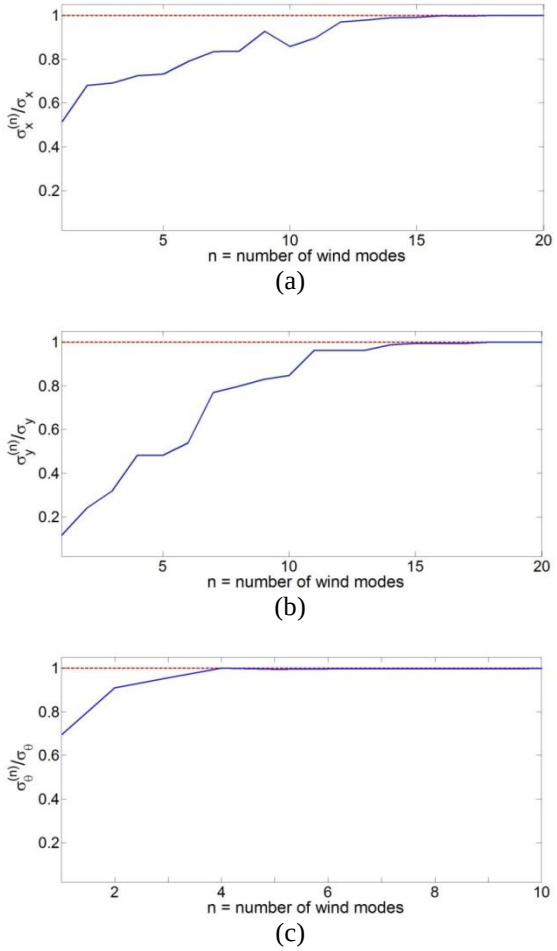

Fig. 4 Displacement in x and y direction and rotation θ at the top floor for angle of attack α = 30°; ratio between standard deviations of top displacement components $\sigma_x^{(n)}$, $\sigma_y^{(n)}$, $\sigma_\theta^{(n)}$ obtained with a truncated model of the wind-loads and the complete one σ_x, σ_y, σ_θ as a function of the number n of wind-modes of the covariance tensor **R** included in the truncated model

The decomposition described above has been applied to the forcing field measured in the CRIACIV wind tunnel for the sample building described in Sect. 2 (Vasta and Sepe 2011).

As an example, Fig. 3 reports the first three wind-modes in case of angle of attack $\alpha = 40°$; only the components F_x, F_y of the wind-modes at each floor, amplified by the corresponding eigenvalue, are included in the representation, and this gives a more effective visualization of the relative weight of the wind-modes that contribute to the forcing process; however torsional component M_z, not included in Fig. 3, were obviously taken into account in the modal projection and in the numerical evaluation of structural response described below.

According to the reduced structural model described in Sect. 2, that only includes three structural modes (first flexural ones along x and y directions and first torsional one), the loading field is described by the time-histories of the modal loads $f_j(t)$, j =1, 2, 3 (Eq. (1)), where, denoted by $\mathbf{F}(t)$ the forcing field and by $\boldsymbol{\varphi}_i$ the i-th structural mode, $f_j(t) = \boldsymbol{\varphi}_j^T \mathbf{F}(t)$.

On the other hand, the forcing field $\mathbf{F}(t)$ can be approximated by means of a linear combination of the wind-modes as described in Eq. (7), truncated to the first n contributions, and the question arises about the level of approximation (i.e., the value of n) required to satisfactorily reproduce the main characteristics of the structural response.

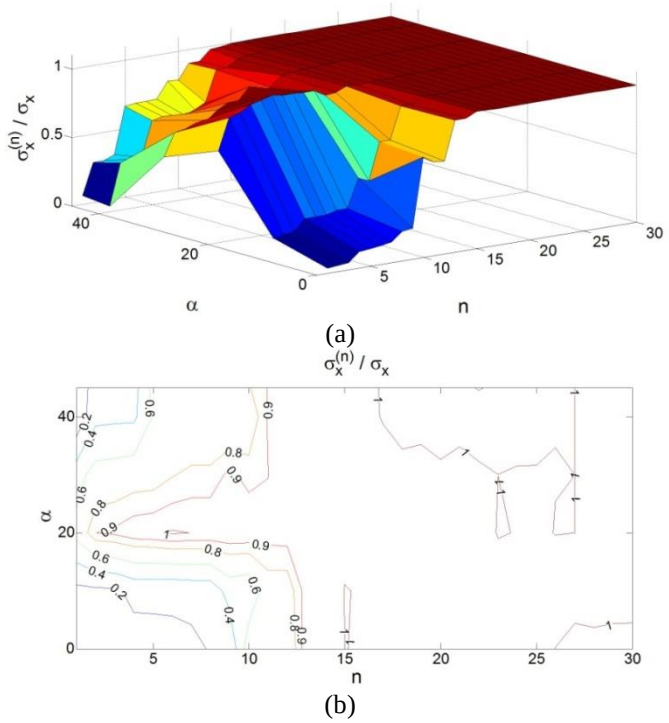

Fig. 5 (a) 3D graph of displacement in x direction at the top floor for several angles of attack α[°]; ratio between standard deviations of top displacement $\sigma_x^{(n)}$ obtained with a truncated model of the wind-loads and the complete one σ_x, as a function of the number n of wind-modes of the covariance tensor **R** included in the truncated model and (b) contour plots

For this reason Eq. (1) has been numerically integrated with software in Matlab environment, for several angles of attach α of the wind and for an increasing number of wind-modes in the decomposition of Eq. (7).

As an example, for the case $\alpha = 30°$ Fig. 4(a) reports the ratio between the standard deviation of the top displacement (74th floor) in the x direction obtained with truncated models of the wind field and the standard deviation of the same displacement corresponding to the complete wind-field, as a function of the number *n* of wind modes considered.

It is evident from the plot of such a ratio that an acceptable approximation of the "real" standard deviation (i.e., the one corresponding to the whole wind field $\mathbf{F}(t)$ acting on the reduced structural model of Eq. (1)) requires, in this example, to include at least a dozen of wind-modes of the covariance tensor **R**.

At least in this case, therefore, and differently from what happens for structural modes, the forcing field cannot be satisfactorily reduced to the contribution of the first few modes, because the higher ones play a not negligible role. A similar trend has been found for top displacements along y, while rotation of the top floor (as an example) seems less sensitive to the number of wind-modes included in the truncated model of the loads, and can be accurately represented even with 4-5 wind-modes (Figs. 4(b)-4(c)).

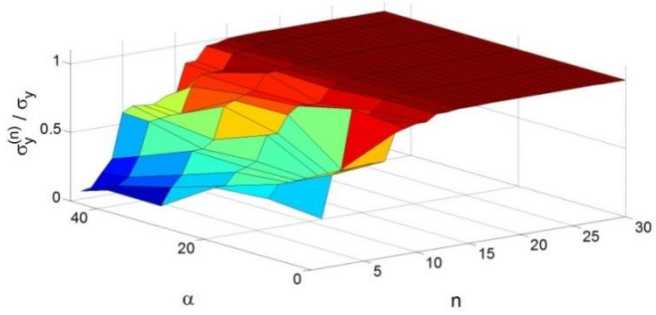

(a)

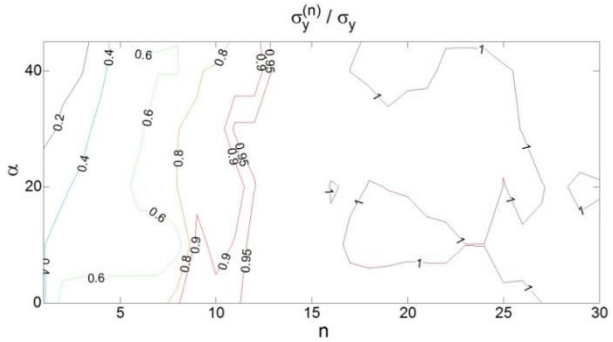

(b)

Fig. 6 (a) 3D graph of displacement in *y* direction at the top floor for several angles of attack $\alpha[°]$; ratio between standard deviations of top displacement $\sigma_y^{(n)}$ obtained with a truncated model of the wind-loads and the complete one σ_y, as a function of the number *n* of wind-modes of the covariance tensor **R** included in the truncated model and (b) contour plots

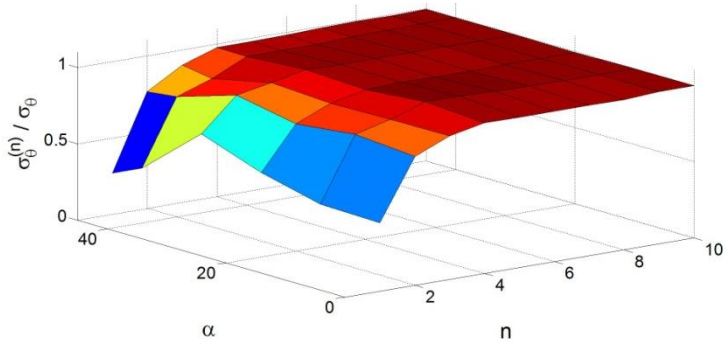

Fig. 7 3D graph of rotation of the top floor for several angles of attack $\alpha[^\circ]$; ratio between standard deviations of top rotation $\sigma_\theta^{(n)}$ obtained with a truncated model of the wind-loads and the complete one σ_θ, as a function of the number n of wind-modes of the covariance tensor **R** included in the truncated model

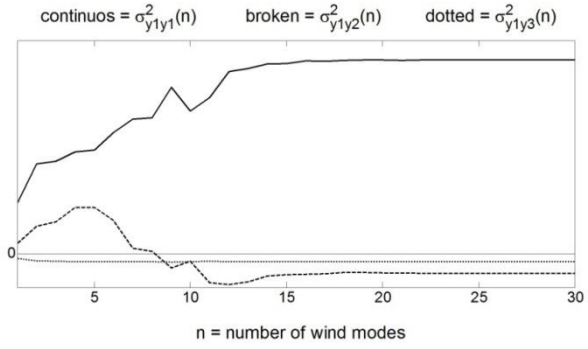

Fig. 8 Ratio between variance $\sigma^2_{y_1y_1}(n)$ and cross-covariances $\sigma^2_{y_1y_1}(n)$, $\sigma^2_{y_1y_3}(n)$ of the amplitudes $y_1(t)$, $y_2(t)$ and $y_3(t)$ of the structural modes obtained with a truncated model of the wind-loads and the complete ones $\sigma^2_{y_1y_1}$, $\sigma^2_{y_1y_2}$, $\sigma^2_{y_1y_3}$ as a function of the number n of wind-modes of the covariance tensor **R** included in the truncated model; angle of attack $\alpha = 30°$

Although no general conclusion can be drawn from the sample cases so far examined, this trend is confirmed for all the different angles of attack considered in the wind-tunnel tests described in Sect. 2; the ratios between standard deviations of top displacements along x and along y for the truncated and the complete model of wind-induced loads for several angles of attack, are reported in Figs. 5(a) and 6(a) respectively (3D representation) and in Figs. 5(b) and 6(b) (contour lines), showing that in general at least 8-10 modes are required to obtain a satisfactorily estimation of the top displacement, while a faster convergence is observed for the rotation of the top floor (Fig. 7).

As shown by Figs. 5, 6, 7, the number of wind modes required for a satisfactory representation of the dynamic structural response significantly depends on the angle of attack α. This aspect, together with the actual wind tunnel setup, can possibly explain some differences between the results discussed here and those reported in Kikuchi *et al*. (1997) about the number and characteristics of wind-modes to be included in a reduced model of the forcing field.

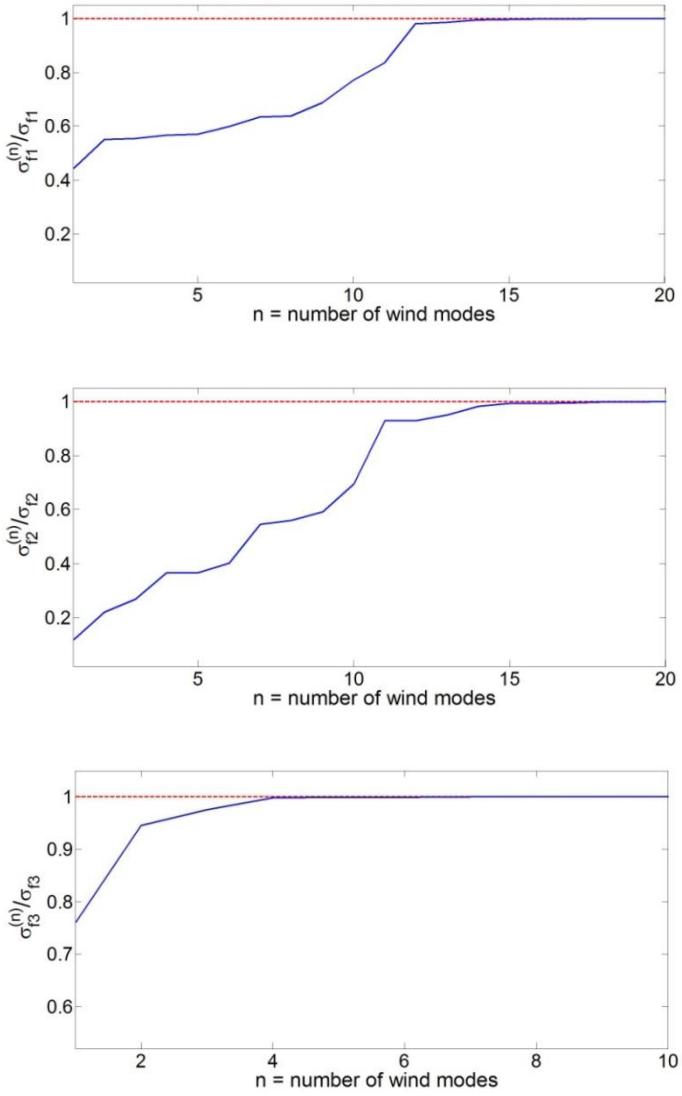

Fig. 9 Ratio between standard deviations $\sigma_{f1}^{(n)}$, $\sigma_{f2}^{(n)}$, $\sigma_{f3}^{(n)}$ of forcing components of the first three structural modes obtained with a truncated model of the wind-loads and the complete ones σ_{f1}, σ_{f2}, σ_{f3} as a function of the number n of wind-modes of the covariance tensor **R** included in the truncated model; angle of attack $\alpha = 30°$

It is also worth to underline that the truncated model of the forcing field is based on wind modes stochastically orthogonal to each other, as described in Sect. 3; however, this does not corresponds, in general, to the orthogonality of the modal components $y_j(t)$ of the structural response (Sect. 2), defined with respect to a different base (structural modes).

This is clearly evident in Fig. 8, where the cross-covariance between some of the modal amplitudes $y_1(t)$, $y_2(t)$ and $y_3(t)$ is shown. As a consequence, the standard deviation of the structural

response may be non monotonically increasing when new wind modes are added (e.g., Fig. 4), while of course a monotonic trend is observed for wind load components, as shown in Fig. 9 (forcing components f_1, f_2, f_3 of the first three structural modes) and Fig. 10 (wind-induced loads F_x, F_y, M_z at the top floor).

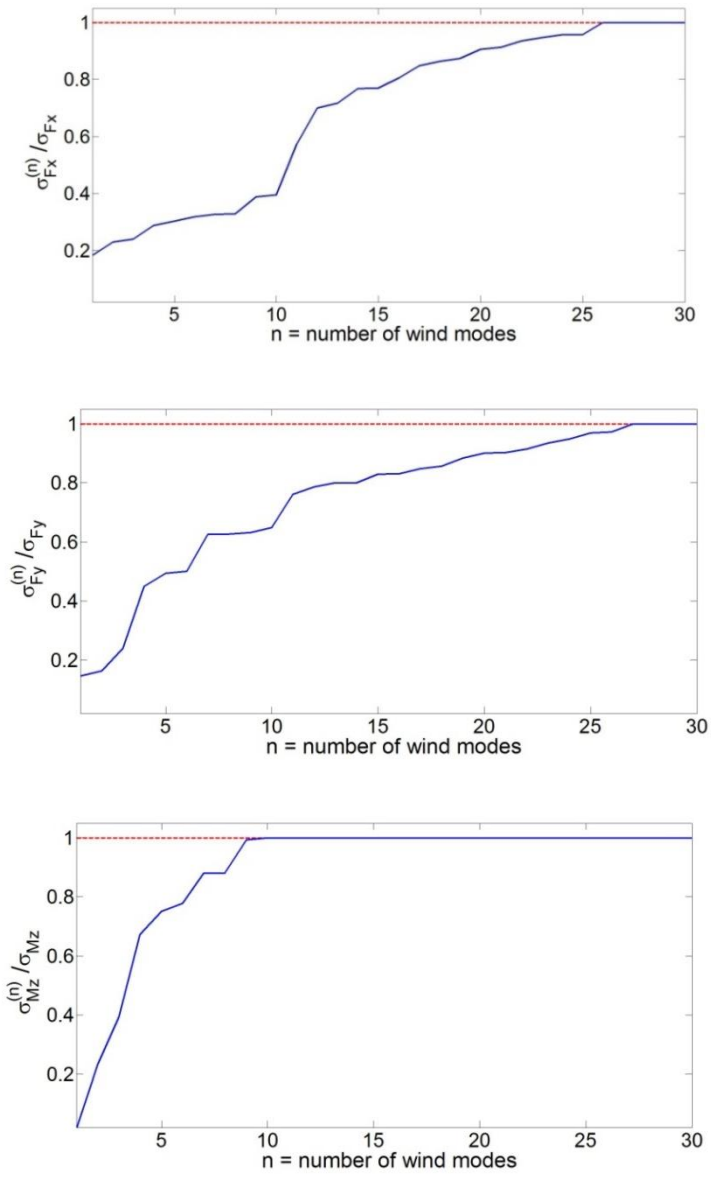

Fig. 10 Ratio between standard deviations $\sigma_{F_x}^{(n)}$, $\sigma_{F_y}^{(n)}$, $\sigma_{M_z}^{(n)}$ of wind-induced loads F_x, F_y, M_z at the top floor obtained with a truncated model of the wind-induced loads and the complete ones $\sigma_{F_x}, \sigma_{F_y}, \sigma_{M_z}$ as a function of the number n of wind-modes of the covariance tensor **R** included in the truncated model; angle of attack $\alpha = 30°$

In the experimental case discussed here it has also been found a faster convergence of the torsional moment M_t compared to the shear forces V_x, V_y and the flexural moment M_2 along wind (i.e., in the mean wind direction, see Fig. 2), as shown by Fig. 11.

In the case here considered, where the measured wind field is deterministically known, the proposed representation of wind loads also allows a detailed reconstruction of the forcing and response time-histories, when an appropriate number of wind modes is taken into account. This is for example shown in Fig. 12 (forcing components $f_1(t)$, $f_2(t)$, $f_3(t)$ of the first three structural modes) and in Fig. 13 (structural displacements $s_x(t)$, $s_y(t)$, $\theta(t)$ at the building top).

4. Reduced model of the wind-induced loads based on the PSD wind-tensor

A more suitable representation of the wind field may be achieved by means of the decomposition in fully coherent independent vectors (Di Paola 1998). Although the non gaussianity of the pressure wind field $\mathbf{F}(t)$, its main characteristics can be represented by the knowledge of the second order spectral properties. To this end, let us consider the PSD matrix of $\mathbf{F}(t)$

$$\mathbf{S}_{\mathbf{F}}(\omega)=\begin{bmatrix} S_{F_1F_1}(\omega) & S_{F_1F_2}(\omega) & \cdots & S_{F_1F_m}(\omega) \\ S_{F_2F_1}(\omega) & S_{F_2}(\omega) & \cdots & S_{F_2F_m}(\omega) \\ \vdots & & \ddots & \vdots \\ S_{F_1F_m}(\omega) & \cdots & \cdots & S_{F_mF_m}(\omega) \end{bmatrix} \tag{10}$$

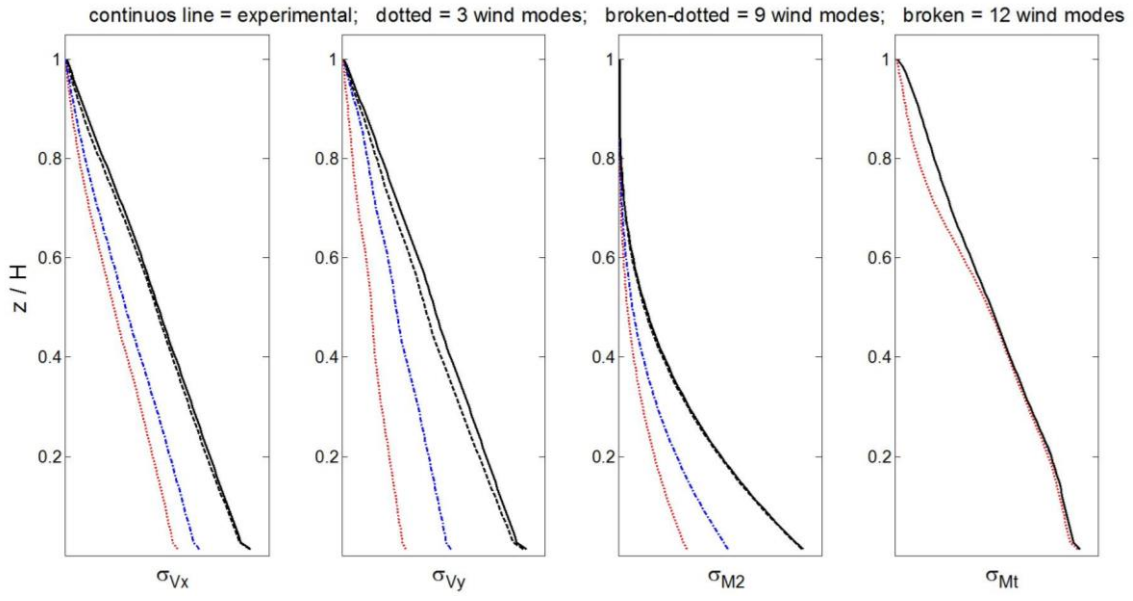

Fig. 11 Standard deviations σ_{V_x}, σ_{V_y}, σ_{M_2}, σ_{M_t} of shear forces V_x and V_y, flexural moment M_2 (direction 2 defined in Fig. 2) and torsional moment M_t along the height of the building for a reduced model with 3, 9 and 12 wind-modes of the covariance tensor **R**, compared with experimental standard deviations; angle of attack $\alpha = 30°$

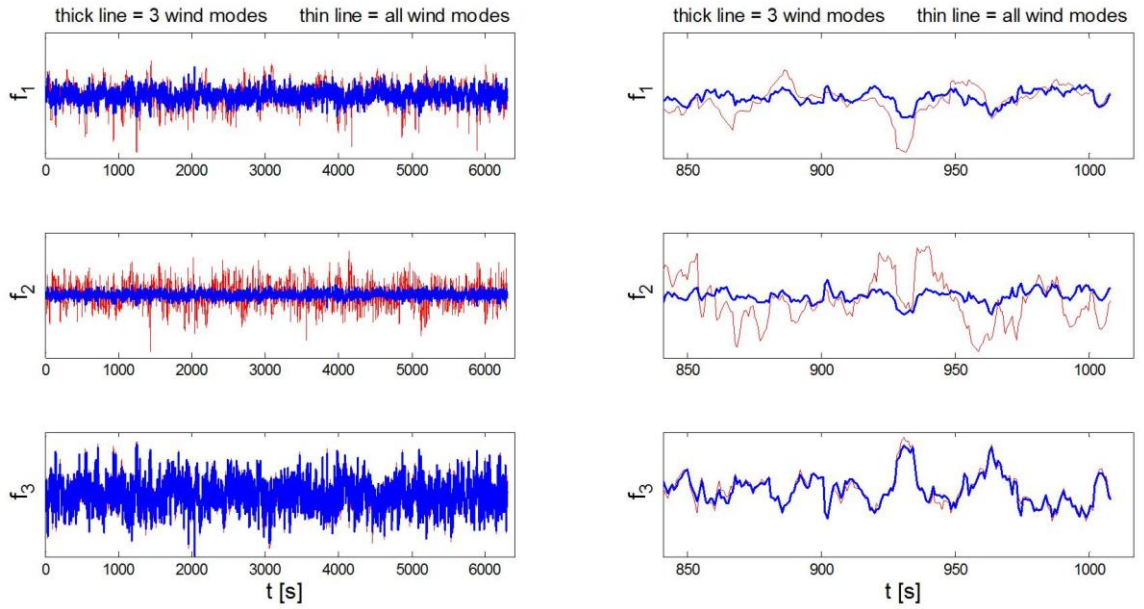

(a)

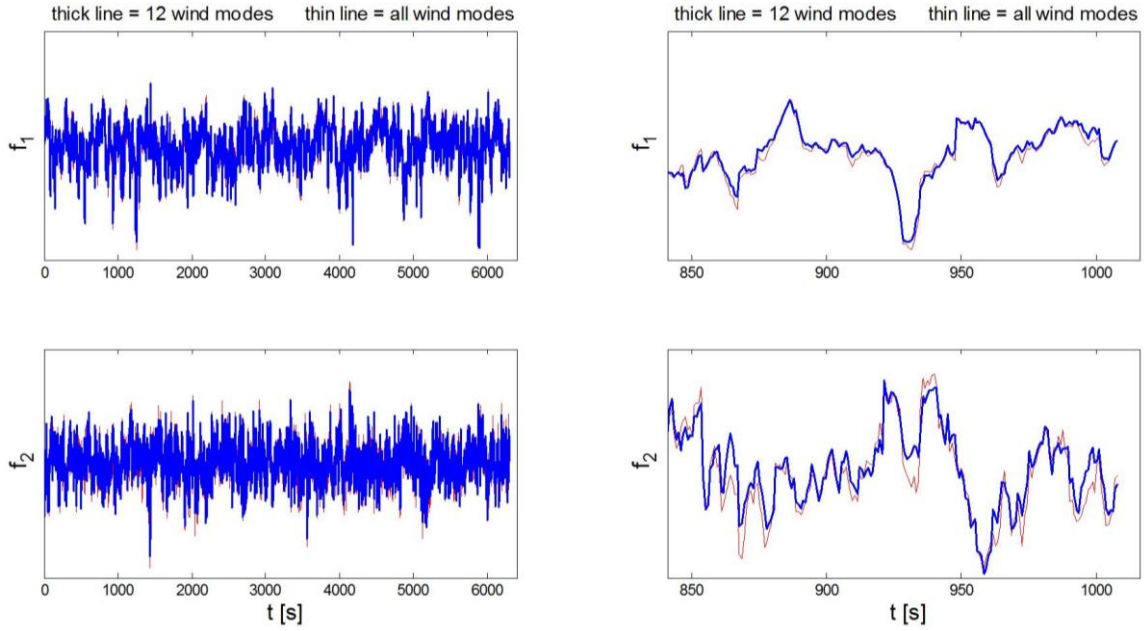

(b)

Fig. 12 Time-history of the forcing components $f_1(t)$, $f_2(t)$, $f_3(t)$ on the first three structural modes reconstructed with truncated models of the wind- induced loads: (a) 3 wind-modes and (b) 12 wind-modes of the covariance tensor **R**; angle of attack $\alpha = 30°$

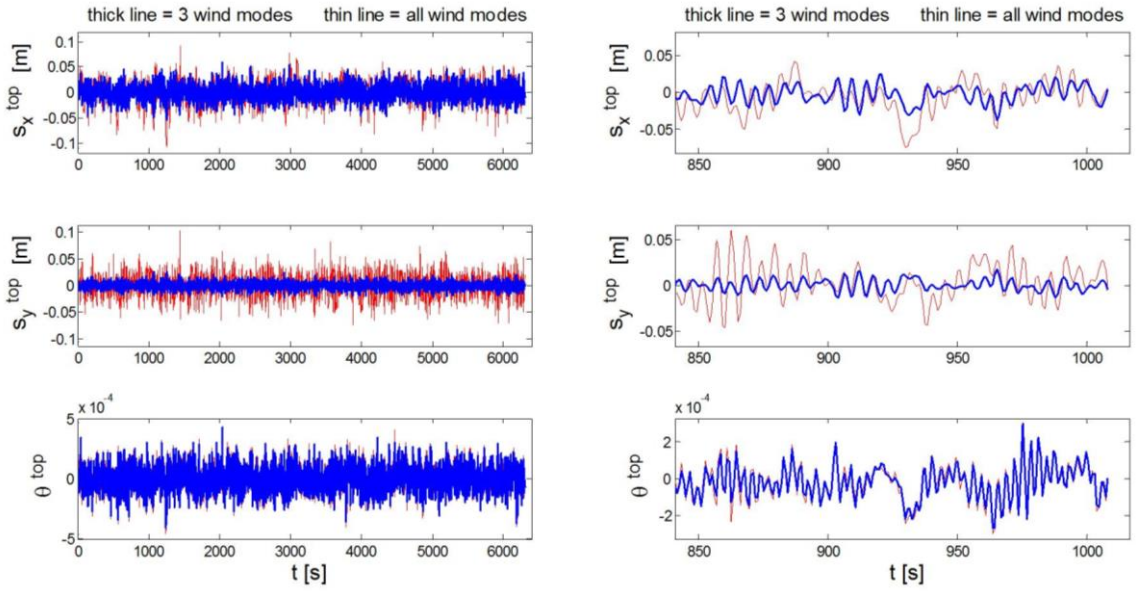

(a)

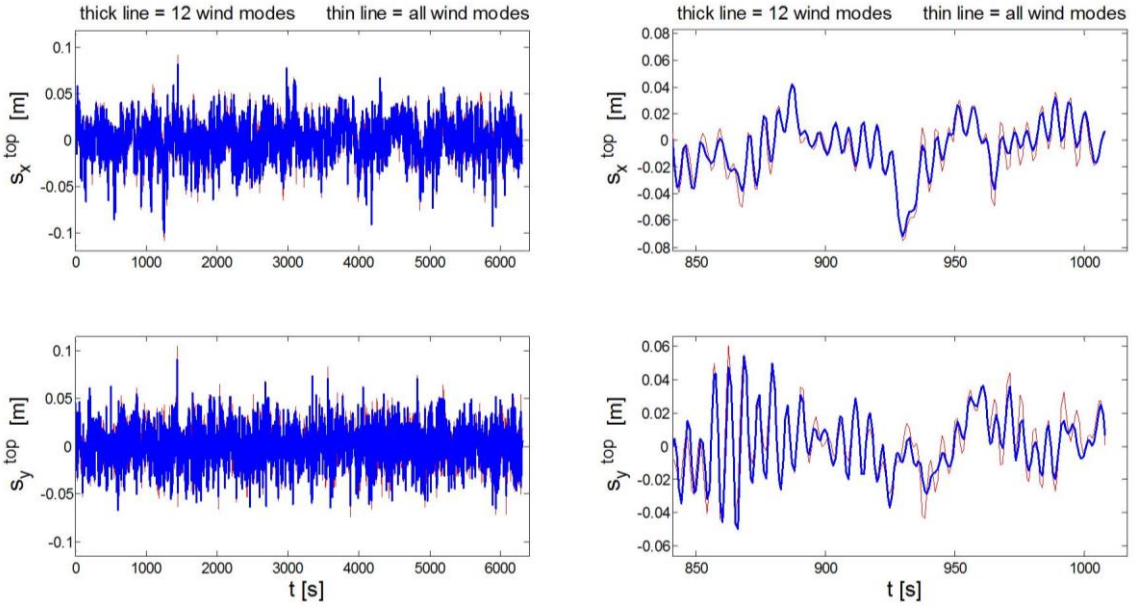

(b)

Fig. 13 Time-history of the structural displacements $s_x(t)$, $s_y(t)$, $\theta(t)$ at the building top reconstructed with truncated models of the wind- induced loads: (a) 3 wind-modes and (b) 12 wind-modes of the covariance tensor **R**; angle of attack $\alpha = 30°$

The elements of $\mathbf{S_F}(\omega)$ are the direct and cross power spectral densities, defined as the Fourier transform of the correlation components

$$S_{F_iF_j}(\omega)=\frac{1}{2\pi}\int_{-\infty}^{+\infty}R_{F_iF_j}(\tau)e^{-j\omega\tau}d\tau$$

or equivalently, starting from measurements of the process $\mathbf{F}(t)$

$$S_{F_iF_j}(\omega)=\frac{1}{2\pi}\lim_{T\to\infty}\frac{E\left[F_i(\omega,T)F_j^*(\omega,T)\right]}{T}$$

where $F_i(\omega,T)$ denotes the Fourier transform of $F_i(t)$ over the observation time T

$$F_i(\omega,T)=\int_0^T F_i(t)e^{-j\omega t}dt$$

The psd matrix is Hermitian and non-negative definite, thus its eigenvalues $\Gamma(\omega)=diag(\gamma_1(\omega)\gamma_2(\omega)\cdots\gamma_m(\omega))$ are real and non-negative, with orthonormal complex eigenvectors $\Psi(\omega)=[\boldsymbol{\psi}_1(\omega)\boldsymbol{\psi}_2(\omega)\cdots\boldsymbol{\psi}_m(\omega)]$

$$\mathbf{S_F}(\omega)\Psi(\omega)=\Psi(\omega)\Gamma(\omega) \tag{11}$$

$$\Psi(\omega)^{*T}\Psi(\omega)=\mathbf{I},\quad \Psi(\omega)^{*T}\mathbf{S_F}(\omega)\Psi(\omega)=\Gamma(\omega) \tag{12}$$

Following (Di Paola 1998) an optimal basis to represent the wind load $\mathbf{F}(t)$ is a linear combination of the spectral wind modes $\boldsymbol{\psi}_k(\omega)$

$$\mathbf{F}(t)=\boldsymbol{\mu}_F+\mathrm{Re}\left(2\sum_{k=1}^{m}\sum_{j=1}^{N}\boldsymbol{\psi}_k(\omega_j)\sqrt{\gamma_k(\omega_j)\Delta\omega}\cdot g_j^{(k)}(t)\right) \tag{13}$$

where N is the number of discretization frequency points and $\Delta\omega$ the integration mesh step size, while

$$g_j^{(k)}(t)=R_j^{(k)}\cos(\omega_j t)+I_j^{(k)}\sin(\omega_j t) \tag{14}$$

In Eq. (13), when digital simulation is performed, $R_j^{(k)}$ and $I_j^{(k)}$ are independent zero mean gaussian distributed variables with variance equal to 1/2 (Di Paola 1998).

It is worth noting that since measurement of $\mathbf{F}(t)$ are known in the sample case here described, the $R_j^{(k)}$ and $I_j^{(k)}$ coefficients may be evaluated as Fourier coefficients of the expansion Eq. (13), because of the orthonormality Eq. (11), as

$$\begin{aligned}R_j^{(k)}&=\mathrm{Re}\left(\frac{\boldsymbol{\psi}_k^{*\mathrm{T}}(\omega_j)}{\sqrt{\gamma_k(\omega_j)\Delta\omega T}}\int_0^{2\pi}[\mathbf{F}(t)-\boldsymbol{\mu}_F]\cos(\omega_j t)dt\right)\\ I_j^{(k)}&=\mathrm{Re}\left(\frac{\boldsymbol{\psi}_k^{*\mathrm{T}}(\omega_j)}{\sqrt{\gamma_k(\omega_j)\Delta\omega T}}\int_0^{2\pi}[\mathbf{F}(t)-\boldsymbol{\mu}_F]\sin(\omega_j t)dt\right)\end{aligned} \tag{15}$$

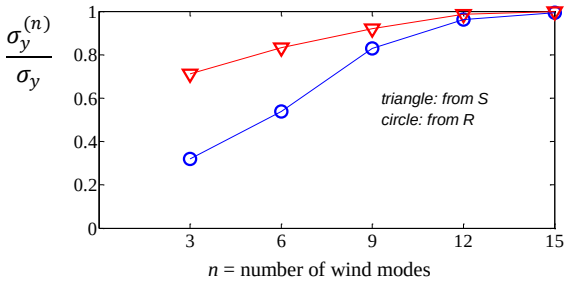

Fig. 14 Comparison between the standard deviations $\sigma_y^{(n)}$ of the displacement in the *y* direction at the top of the structure obtained with SPT (tensor **S**) or CPT (tensor **R**) truncated models, as a function of the number *n* of wind-modes included in the truncated model; σ_y denotes the standard deviation of displacement obtained with a complete wind model

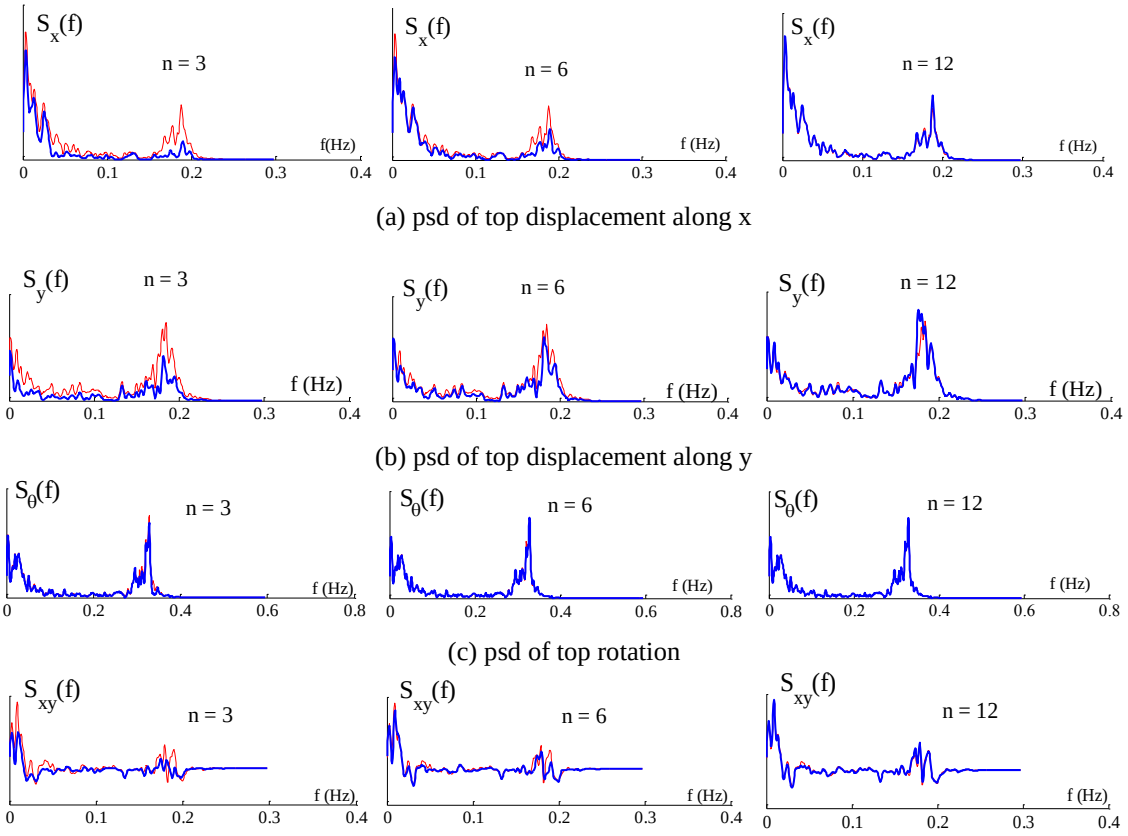

(a) psd of top displacement along x

(b) psd of top displacement along y

(c) psd of top rotation

(d) cpsd of top displacements along x and y

Fig. 15 Power spectral density (psd) and cross power spectral density (cpsd) of displacement components at the building top, for a reduced model of the wind-induced loads based on the **PSD wind-tensor** (Sect. 4); approximate solution (thick curve) for a truncated model with n = 3, 6, 12 blowing-modes, compared with the exact solution (thin curve) for a complete wind model

If the eigenvalues are sorted in decreasing order, then the summation in Eq. (13) can be truncated considering only a limited number of principal components.

In the case here described, the reduced model obtained in this way (known as spectral proper transformation, SPT, (Carassale *et al.* 2007, Solari *et al.* 2007) turns out to be more efficient with respect to the reduced model of Sect. 3 (covariance proper transformation, CPT), in the sense that a lower number of blowing-modes is needed to reproduce the effect of the measured wind field.

This is shown in Fig. 14, where the standard deviations of top displacements obtained with SPT or CPT truncated models are compared. The higher efficiency of SPT with respect to CPT is also shown by the comparison of psd and cpsd curves reported in Fig. 15 (SPT) and Fig. 16 (CPT), where the approximate solution (thick curve) is compared with the exact solution (thin curve) for 3, 6 or 12 blowing-modes.

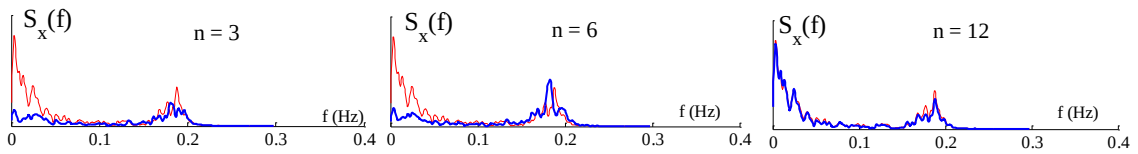

(a) psd of top displacement along x

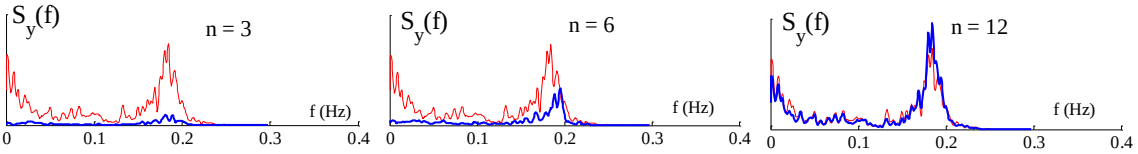

(b) psd of top displacement along y

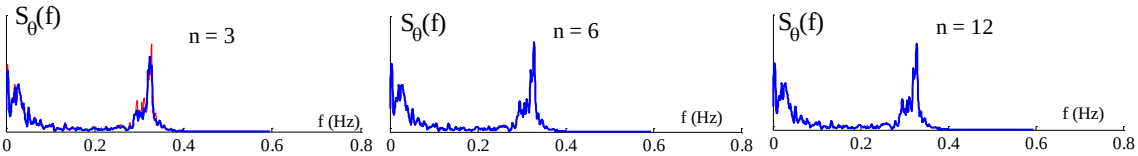

(c) psd of top rotation

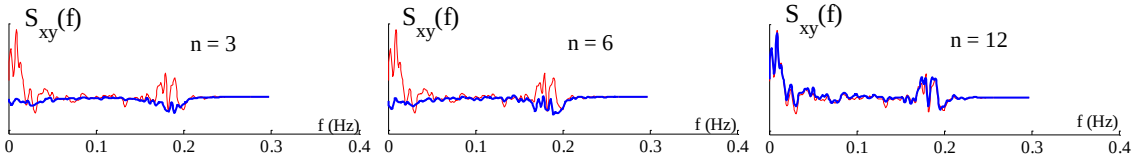

(d) cpsd of top displacements along x and y

Fig. 16 Power spectral density (psd) and cross power spectral density (cpsd) of displacement components at the building top, for a reduced model of the wind-induced loads based on the **covariance wind-tensor** (Sect. 3); approximate solution (thick curve) for a truncated model with n = 3, 6, 12 blowing-modes, compared with the exact solution (thin curve) for a complete wind model

5. Conclusions

Starting from the well accepted representation of the wind field by means of *blowing modes* (or *wind modes*), i.e., coherent wind fields characterized by highest energetic weights and stochastically orthogonal to each other an investigation has been performed in this paper for the case of high-rise buildings; the investigation described here is based on experimental results obtained on a in-scale model by researchers of Florence and Perugia Universities in the boundary-layer wind tunnel of CRIACIV (Inter-University Research Centre on Building Aerodynamics and Wind Engineering) in Prato (Italy).

Aiming to obtain a reduced model for the wind field, the paper describes an algorithm that extracts the wind-modes from the covariance matrix of the forcing time-histories, and represents them by means of a very expressive 3D representation.

As discussed in the paper, the elaboration of experimental data shows that the multi-correlated field of wind-induced loads cannot in general be reduced to the contribution of the first few blowing modes of the covariance wind-tensor, because higher modes can play a non-negligible role.

A more efficient reduction of the wind field is instead obtained when eigenvectors of the power spectral density tensor are used in the reduced model of wind-induced loads.

The two alternative representations are in fact not equivalent, because SPT fully decorrelates the principal components, while PCA decorrelates them only for $\tau = 0$. However their physical implications are still under investigation and the question of optimal representation of stationary multi-variate random processes remains open.

Acknowledgments

This work has been developed in the framework of the research project "*Wind effects on slender structures: Performance-based Optimal Design (Wi-POD)*", financially supported in 2007 by the Italian Ministry for University and Research and by five Italian Universities.

Prof. Gianni Bartoli, Prof. Massimiliano Gioffré and Dr. Seymour M.J. Spence of CRIACIV (Inter-University Research Centre on Building Aerodynamics and Wind Engineering) are deeply acknowledged for making available the data of wind tunnel tests.

References

Bellizzotti, G., Sepe, V. and Vasta, M. (2010), "Reduced models for wind-induced loads and structural response", *Proceedings of the 11th Italian Conference on Wind Engineering IN-VENTO-2010*, Spoleto (Italy), June-July 2010 (*in Italian*).

Carassale, L. (2005), "POD-based filters for the representation of random loads on structures", *Probabilist. Eng.Mech.*, **20**(3), 263-280.

Carassale, L. and Marré Brunenghi, M. (2011), "Statistical analysis of wind-induced pressure fields: a methodological perspective", *J. Wind Eng. Ind. Aerod.*, **99**(6-7), 700-710

Carassale, L. and Marré Brunenghi, M. (2012), "Identification of meaningful coherent structures in the wind-induced pressure on a prismatic body", *J. Wind Eng. Ind. Aerod.*, **104-106**, 216-226

Carassale, L., Solari, G. and Tubino, F. (2007), "Proper orthogonal decomposition in wind engineering. Part 2: theoretical aspects and some applications", *Wind Struct.*, **10**(2), 177-208

Cluni, F., Gusella, V., Spence, S.M.J. and Bartoli, G. (2011), "Influence of the wind load correlation on the estimation of the generalised forces for 3D coupled tall buildings", *J. Wind Eng. Ind. Aerod.*, **99**(7), 682-690

Di Paola, M. (1998), "Digital simulation of wind velocity", *J. Wind Eng. Ind. Aerod.*, **74-76**, 91-109.

Ghanem, R. and Spanos, P. (1991), *Stochastic finite elements: a spectral approach*, Springer-Verlag, New York, Berlin, Heidelberg.

Holmes, J.D., Sankaran, R., Kwok K.C.S. and Syme M.J. (1997), "Eigenvector modes of fluctuating pressures on low-rise building models", *J. Wind Eng. Ind. Aerod.*, **69-71**, 697-707.

Honerkamp, J. (1994), *Stochastic dynamical systems*, VCH, New York.

Kho, S., Baker, C. and Hoxey, R. (2002), "POD/ARMA reconstruction of the surface pressure field around a low rise structure", *J. Wind Eng. Ind. Aerod.*, **90**(12-15), 1831-1842.

Kikuchi, H., Tamura, Y., Ueda, H. and Hibi, K. (1997), "Dynamic wind pressures acting on a tall building model - proper orthogonal decomposition", *J. Wind Eng. Ind. Aerod.*, **69-71**, 631-646.

Loeve, M. (1978), *Probability theory II*, Springer, New York, Heidelberg.

Solari, G., Carassale, L. and Tubino, F. (2007), "Proper orthogonal decomposition in wind engineering. Part 1: a state-of-the-art and some prospects", *Wind Struct.*, **10**(2), 153-176

Spence, S.M.J. (2009), *Time domain Non-Gaussian optimization of wind excited tall buildings under vulnerability constraints*, Ph.D. Dissertation, University of Firenze (Italy) and Technische Universität "Carolo Wilhelmina" of Braunschweig (Germany)

Spence, S.M.J., Bernardini, E. and Gioffré, M. (2011), "Influence of the wind load correlation on the estimation of the generalised forces for 3D coupled tall buildings", *J. Wind Eng. Ind. Aerod.*, **99**, 757-766

Spence, S.M.J., Gioffré, M. and Gusella, V. (2008), "Influence of higher modes on the dynamic response of irregular and regular tall buildings", *Proceedings of the 6th International Colloquium on Bluff Bodies Aerodynamics and Applications (BBAA VI)*, Milano, Italy, July 20-24.

Tamura, Y., Suganuma, S., Kikuchi, H. and Hibi, K. (1999), "Proper orthogonal decomposition of random wind pressure field", *J. Fluid. Struct.*, **13**(7-8), 1069-1095.

Tamura, Y., Ueda, H., Kikuchi, H., Hibi, K., Suganuma, S. and Bienkiewicz, B. (1997), "Proper orthogonal decomposition study of approach wind-building pressure correlation", *J. Wind Eng. Ind. Aerod.*, **72**, 421-432.

Vasta, M. and Sepe, V. (2011), "Reduced models for wind-induced loads and structural response: wind-tunnel experimental tests", *Proceedings of the 8th European Conference on Structural Dynamics EURODYN 2011*, Leuven, Belgium, July 4-6.

Vasta, M. and Schueller, G.I. (2000), "Stochastic phase space reduction of non linear systems by Karhunen Loeve expansion", *J. Eng. Mech. - ASCE*, **126**(6), 626-632.

Yamazaki, F., Shinozuka, M. and Dasgupta, G. (1988), "Neumann expansion for stochastic finite-element analysis", *J. Eng. Mech. - ASCE*, **114**(8), 1335-1354.

Yamazaki, F. and Shinozuka, M. (1990), "Simulation of stochastic fields by statistical preconditioning", *J. Eng. Mech. - ASCE*, **116** (2), 268-287.

CC